

## Research Article

# Effect of Caffeine- $\text{Zn}^{2+}$ System in Preventing Corrosion of Carbon Steel in Well Water

K. Rajam,<sup>1</sup> S. Rajendran,<sup>2,3</sup> and N. Nazeera Banu<sup>3</sup>

<sup>1</sup> Department of Chemistry, K. L. N. College of Information Technology, Pottapalayam 630 611, India

<sup>2</sup> PG and Research Department of Chemistry, GTN Arts College, Dindigul 624 005, India

<sup>3</sup> Department of Chemistry, RVS School of Engineering and Technology, Dindigul 624 005, India

Correspondence should be addressed to K. Rajam; [rajam98@yahoo.co.in](mailto:rajam98@yahoo.co.in)

Received 19 June 2012; Revised 18 October 2012; Accepted 18 October 2012

Academic Editor: Deniz Ekinici

Copyright © 2013 K. Rajam et al. This is an open access article distributed under the Creative Commons Attribution License, which permits unrestricted use, distribution, and reproduction in any medium, provided the original work is properly cited.

The inhibition efficiency (IE) of caffeine in controlling corrosion of carbon steel in well water in the absence and presence of  $\text{Zn}^{2+}$  has been evaluated by mass loss method. The formulation, consisting of 200 ppm of caffeine and 50 ppm  $\text{Zn}^{2+}$ , offers 82% inhibition efficiency to carbon steel immersed in well water. Addition of malic acid increases inhibition efficiency of the caffeine- $\text{Zn}^{2+}$  system. The inhibition efficiency of caffeine- $\text{Zn}^{2+}$  and caffeine- $\text{Zn}^{2+}$ -malic acid system decreases with the increase in immersion period and increases with the increase in pH from 3 to 11. AC impedance spectra, SEM micrographs, and AFM studies reveal the formation of protective film on the metal surface. The film is found to be UV fluorescent.

## 1. Introduction

The environmental friendly nontoxic, biodegradable, and readily available natural products have been used widely as corrosion inhibitors. Many heterocyclic compounds such as Pyridine [1–3], triazoles [4–9] have been used as inhibitors. It was reported that Plant extracts such as Cerum Petroselinum, Doum, and orange shells [10] are used as inhibitors. Rajendran et al. [11, 12] have evaluated the inhibition efficiency of various concentrations of caffeine- $\text{Zn}^{2+}$  system in controlling the corrosion of mild steel immersed in aqueous solution containing 60 ppm of  $\text{Cl}^-$ . Rajendran et al. [13] have investigated the inhibition efficiency of caffeine in suppressing the corrosion of carbon steel immersed in 60 ppm of  $\text{Cl}^-$  environment in the absence and presence of  $\text{Mn}^{2+}$ . The synergistic effect of Sebacate with benzotriazole [14] as inhibitor has been studied. Hence there is a search for the nontoxic, ecofriendly corrosion inhibitors. The inhibition performance of carbon steel has been studied by Yesu et al. [15]. Caffeine as a nontoxic material and an alkaloid [16] is chosen as the corrosion inhibitor for this study along with  $\text{Zn}^{2+}$  as coinhibitor. Caffeine as an alkaloid and nontoxic material is chosen as the corrosion inhibitor for this present study along with zinc ions.

The present work is undertaken:

- (i) to evaluate the inhibition efficiency (IE) of caffeine in controlling the corrosion of carbon steel in well water in the absence and presence of  $\text{Zn}^{2+}$ ,
- (ii) to evaluate the influence of malic acid, duration of immersion, and pH on the IE of the caffeine- $\text{Zn}^{2+}$  and caffeine- $\text{Zn}^{2+}$ -malic acid systems,
- (iii) to analyse the protective film on carbon steel by Scanning Electron Microscopy and Atomic Force Microscopy,
- (iv) to study the mechanistic aspects by AC impedance study, and
- (v) to propose a suitable mechanism for corrosion inhibition.

## 2. Experimental Procedure

**2.1. Preparation of Specimens.** Carbon steel specimens (0.0267% S, 0.06% P, 0.4% Mn, 0.1% C and the rest iron) of dimensions 1.0 cm × 4.0 cm × 0.2 cm were polished to a mirror finish and degreased with trichloroethylene.

TABLE 1: Parameters of well water.

Parameter	Value
pH	8.6
Conductivity	2620 $\mu\text{mho/cm}$
TDS	1835 mg/L
Chloride	450
Sulphate	110
Total hardness	96

**2.2. Mass Loss Method.** Relevant data on the well water used in this study are given in Table 1. Carbon steel specimens in triplicate were immersed in 100 mL of the solutions containing various concentrations of the inhibitor in the presence and absence of  $\text{Zn}^{2+}$  for 3 days. The weight of the specimens before and after immersion was determined using Shimadzu balance, model AY 62. The corrosion products were cleansed with Clarke's solution [17]. The inhibition efficiency (IE) was then calculated using the equation

$$\text{IE} = 100 \left[ 1 - \left( \frac{W_2}{W_1} \right) \right] \%, \quad (1)$$

where  $W_1$  is the corrosion rate in the absence of the inhibitor and  $W_2$  is the corrosion rate in the presence of the inhibitor.

**2.3. AC Impedance Measurements.** AC impedance studies were carried out in an H&CH electrochemical work station impedance analyzer model CHI 660 A. A three electrode cell assembly was used. The working electrode was carbon steel. A saturated calomel electrode (SCE) was used as the reference electrode and a rectangular platinum foil was used as the counter electrode. The real part and the imaginary part of the cell impedance were measured in ohms at various frequencies. The values of charge transfer resistance,  $R_t$ , and the double layer capacitance,  $C_{dl}$ , were calculated.

**2.4. Atomic Force Microscopy (AFM).** Samples were scanned at various scan areas using a Shimadzu SPM 9500-21 Scanning Probe Microscope. For high resolution, contact mode microcantilever was used for all analyses. Digital images were stored in computer and processed.

**2.5. Fluorescence Spectra.** These spectra were recorded in a Hitachi F-4500 fluorescence Spectrophotometer.

### 3. Results and Discussion

**3.1. Analysis of Results of Mass Loss Method.** The corrosion rate (CR) of carbon steel immersed in well water (whose composition is given in Table 1) in the absence and presence of inhibitor systems are given in Table 2. The inhibition efficiencies (IE) are also given in the Table 2. It is seen from Table 2 that 50 ppm of caffeine shows an IE of 2%. Further addition of caffeine increases the IE and 250 ppm of caffeine exhibits an IE of 13%. Hence caffeine itself is not a good inhibitor. However the combination of caffeine and  $\text{Zn}^{2+}$  shows better IE.

**3.1.1. Influence of  $\text{Zn}^{2+}$  on the Inhibition Efficiency of Caffeine.** The influence of  $\text{Zn}^{2+}$  on the IE of caffeine is given in Table 2. In the presence of  $\text{Zn}^{2+}$  excellent inhibitive property is shown by caffeine. 200 ppm of caffeine and 50 ppm of  $\text{Zn}^{2+}$  shows the IE of 82%. This is found to be the maximum IE offered by the system [18, 19].

**3.1.2. Influence of Malic Acid on the Inhibition Efficiency of Caffeine (200 ppm)- $\text{Zn}^{2+}$  (50 ppm) System.** The influence of malic acid on the IE of caffeine (200 ppm)- $\text{Zn}^{2+}$  (50 ppm) system is given in Table 3. It is interesting to find that the IE of the caffeine- $\text{Zn}^{2+}$  system is increased by the addition of malic acid [20, 21].

**3.1.3. Influence of Duration of Immersion on the IE of Caffeine (200 ppm)- $\text{Zn}^{2+}$  (50 ppm) and Caffeine (200 ppm)- $\text{Zn}^{2+}$  (50 ppm)-Malic Acid (25 ppm) System.** The influence of duration of immersion on the IE of caffeine (200 ppm)- $\text{Zn}^{2+}$  (50 ppm) and caffeine (200 ppm)- $\text{Zn}^{2+}$  (50 ppm)-malic acid (25 ppm) system is given in Tables 4 and 5. It is found that as the immersion period increases IE decreases. The protective film formed on the surface is broken. That is the protective film formed on the surface goes into the solution as the immersion period increases [22].

**3.1.4. Influence of Duration of pH on the IE of Caffeine (200 ppm)- $\text{Zn}^{2+}$  (50 ppm) and Caffeine (200 ppm)- $\text{Zn}^{2+}$  (50 ppm)-Malic Acid (25 ppm) System.** The influence of pH on the IE of caffeine (200 ppm)- $\text{Zn}^{2+}$  (50 ppm) and caffeine (200 ppm)- $\text{Zn}^{2+}$  (50 ppm)-malic acid (25 ppm) system is given in Tables 6 and 7. It is found that at lower pH, IE decreases. The protective film formed on the surface is broken by  $\text{H}^+$  ions of the acid.

**3.2. Analysis of the Results of AC Impedance Spectra.** The AC impedance spectra of carbon steel immersed in various solutions are shown in Figures 1(a), 1(b), and 1(c) (Nyquist plots) and Figures 2(a), 2(b), and 2(c) (Bode plots). The AC impedance parameters, namely, charge transfer resistance ( $R_t$ ) and double layer capacitance ( $C_{dl}$ ) are given in Table 8. When carbon steel is immersed in well water  $R_t$  value is  $1377 \Omega \text{ cm}^2$  and  $C_{dl}$  value is  $3.7005 \times 10^{-9} \text{ F cm}^{-2}$ . When caffeine and  $\text{Zn}^{2+}$  are added to well water,  $R_t$  value increases from  $1377 \Omega \text{ cm}^2$  to  $4435 \Omega \text{ cm}^2$ . The  $C_{dl}$  decreases from  $3.7005 \times 10^{-9} \text{ F cm}^{-2}$  to  $2.6617 \times 10^{-9} \text{ F cm}^{-2}$ . The impedance value (Log  $Z/\text{ohm}$ ) increases from 3.28 to 3.34. Similarly when malic acid is added to caffeine and  $\text{Zn}^{2+}$  system the  $R_t$  value increased to  $2499 \Omega \text{ cm}^2$ , the  $C_{dl}$  decreased to  $2.0390 \times 10^{-9} \text{ F cm}^{-2}$  and the impedance value (Log  $Z/\text{ohm}$ ) increased to 3.47. This suggests that a protective film is formed on the surface of the metal [23, 24].

**3.3. Analysis of the Results of Atomic Force Microscopy.** Atomic force microscopy is a powerful technique for the gathering of roughness statistics from a variety of surfaces.

TABLE 2: Corrosion rate (CR) of carbon steel immersed in well water, in the absence and presence of inhibitors, and the inhibition efficiency (IE) obtained by mass loss method.

Caffeine (ppm)	Zn <sup>2+</sup>					
	0 (ppm)		25 (ppm)		50 (ppm)	
	CR (mdd)	IE (%)	CR (mdd)	IE (%)	CR (mdd)	IE (%)
0	22.42	—	20.18	10	19.73	12
50	21.97	02	12.33	45	11.66	48
100	20.85	07	11.66	48	9.87	56
150	20.18	10	9.87	56	7.85	65
200	19.73	12	8.97	60	4.04	82
250	19.51	13	4.71	79	4.04	82

TABLE 3: Influence of malic acid on IE of caffeine (200 ppm)-Zn<sup>2+</sup> (50 ppm).

Caffeine (ppm)	Zn <sup>2+</sup> (ppm)	Malic acid (ppm)	CR (mdd)	IE (%)
0	0	0	22.42	—
200	50	5	3.59	84
200	50	10	2.92	87
200	50	15	2.24	90
200	50	20	1.79	92
200	50	25	1.35	94

TABLE 4: Influence of duration of immersion on IE of caffeine (200 ppm)-Zn<sup>2+</sup> (50 ppm).

System	Immersion period (days)	CR (mdd)		IE (%)
		Presence of inhibitor	Absence of inhibitor	
Caffeine (200 ppm)-Zn <sup>2+</sup> (50 ppm)	1	2.04	20.40	90
	3	4.04	22.42	82
	5	55.14	68.92	20
	7	80.16	93.21	14

TABLE 5: Influence of duration of immersion on IE of caffeine (200 ppm)-Zn<sup>2+</sup> (50 ppm), malic acid (25 ppm).

System	Immersion period (days)	CR (mdd)		IE (%)
		Presence of inhibitor	Absence of inhibitor	
Caffeine (200 ppm)-Zn <sup>2+</sup> (50 ppm), malic acid (25 ppm).	1	1.02	20.40	95
	3	2.47	22.42	89
	5	49.62	68.92	28
	7	75.50	93.21	19

AFM is becoming an accepted method of roughness investigation. All atomic force microscopy images were obtained on (PICOSPM 1, Molecular Imaging, and USA make) AFM instrument operating in contact mode in air. The scan size of all the AFM images are  $5\ \mu\text{m} \times 5\ \mu\text{m}$  areas at a scan rate of 2.4 lines per second.

The two-dimensional, three-dimensional AFM morphologies and the AFM cross-sectional profile for polished carbon steel surface (reference sample), carbon steel surface immersed in well water (blank sample), and carbon steel surface immersed in well water containing caffeine (200 ppm)-Zn<sup>2+</sup> (50 ppm) & caffeine (200 ppm)-Zn<sup>2+</sup> (50 ppm)-malic acid (25 ppm) are shown in Figures 3(a)–3(d), 3(e)–3(h), and 3(i)–3(l), respectively.

**3.4. Root-Mean-Square Roughness, Average Roughness and Peak-to-Valley Values.** AFM image analysis was performed

to obtain the average roughness,  $R_a$  (the average deviation of all points roughness profile from a mean line over the evaluation length), root-mean-square roughness,  $R_q$  (the average of the measured height deviations taken within the evaluation length and measured from the mean line) and the maximum peak to valley (P-V) height values (largest single peak-to-valley height in five adjoining sampling heights).  $R_q$  is much more sensitive than  $R_a$  to large and small height deviations from the mean [22, 25].

Table 9 is a summary of the average roughness  $R_a$ , rms roughness  $R_q$ , maximum peak-to-valley height (P-V) value for carbon steel surface immersed in different environments. The value of  $R_q$ ,  $R_a$ , and P-V height for the polished carbon steel surface (reference sample) are 30 nm, 136 nm, and 280 nm, respectively. This shows that the surface is more homogenous, with some places where the height is lower than the average depth. Figures 3(a), 3(e), and 3(i) displays the

TABLE 6: Influence of pH on IE of caffeine (200 ppm)-Zn<sup>2+</sup> (50 ppm).

System	pH	CR (mdd)		IE (%)
		Presence of inhibitor	Absence of inhibitor	
Caffeine (200 ppm)-Zn <sup>2+</sup> (50 ppm)	3	79.70	88.56	10
	5	43.45	72.41	40
	7	14.62	52.23	72
	8	4.04	22.42	82
	11	0.22	10.81	98

TABLE 7: Influence of pH on IE of caffeine (200 ppm)-Zn<sup>2+</sup> (50 ppm)-malic acid (25 ppm).

System	pH	CR (mdd)		IE (%)
		Presence of inhibitor	Absence of inhibitor	
Caffeine (200 ppm)-Zn <sup>2+</sup> (50 ppm)-malic acid (25 ppm).	3	71.73	88.56	19
	5	49.24	72.41	32
	7	24.55	52.23	53
	8	8.97	22.42	60
	11	1.30	10.81	88

TABLE 8: Corrosion parameters of carbon steel immersed in well water in the absence and presence of inhibitors.

System	Nyquist plot		Bode plot
	$R_t$ Ohm cm <sup>2</sup>	$C_{dl}$ F/cm <sup>2</sup>	Impedance value Log (Z/ohm)
Well water	1377	$3.7005 \times 10^{-9}$	3.28
Caffeine (200 ppm)-Zn <sup>2+</sup> (50 ppm)	4435	$2.6617 \times 10^{-9}$	3.34
Caffeine (200 ppm)-Zn <sup>2+</sup> (50 ppm)-malic acid (25 ppm)	2499	$2.0390 \times 10^{-9}$	3.47

TABLE 9: AFM data for carbon steel immersed in inhibited and uninhibited environments.

Samples	RMS ( $R_q$ )	Average ( $R_a$ )	Maximum
	Roughness (nm)	Roughness (nm)	peak-to-valley height (nm)
Polished carbon steel (control)	30	136	280
Carbon steel immersed in well water (blank)	194	853	1725
Carbon steel immersed in well water + caffeine (200 ppm)-Zn <sup>2+</sup> (50 ppm)	117	464	972
Carbon steel immersed in well water + caffeine (200 ppm)-Zn <sup>2+</sup> (50 ppm)-malic acid (25 ppm)	155	612	1220

noncorroded metal surface. The slight roughness observed on the polished carbon steel surface is due to atmospheric corrosion. The rms roughness, average roughness, and P-V height values for the carbon steel surface immersed in well water are 194 nm, 853 nm, and 1725 nm, respectively. These values suggest that carbon steel surface immersed in well water has a greater surface roughness than the polished metal surface, indicating that the unprotected carbon steel surface is rougher and were due to the corrosion of carbon steel in well water environment. Figures 3(b), 3(e), and 3(i) displays corroded metal surface with few pits.

The formulation consisting of caffeine (200 ppm)-Zn<sup>2+</sup> (50 ppm) in well water shows  $R_q$  value of 117 nm and the average roughness is significantly reduced to 464 nm when compared with 853 nm for carbon steel surface immersed in well water. The maximum peak to valley height was also reduced to 972 nm. Similarly for the system consisting of caffeine (200 ppm)-Zn<sup>2+</sup> (50 ppm)-malic acid (25 ppm) in

well water shows  $R_q$  value of 155 nm and the average roughness is significantly reduced to 612 nm when compared with 853 nm for carbon steel surface immersed in well water. The maximum peak to valley height was also reduced to 1220 nm. These parameters confirm that the surface appears smoother. The smoothness of the surface is due to the formation of a protective film of Fe<sup>2+</sup>-caffeine complex and Zn(OH)<sub>2</sub> on the metal surface thereby inhibiting the corrosion of carbon steel. The above parameters are also somewhat greater than the AFM data of polished metal surface which confirms the formation of film on the metal surface, which is protective in nature.

**3.5. SEM Analysis of Metal Surface.** SEM provides a pictorial representation of the surface. To understand the nature of the film in the absence and presence of inhibitors and the extent of corrosion of carbon steel, the SEM micrographs of the surface are examined.

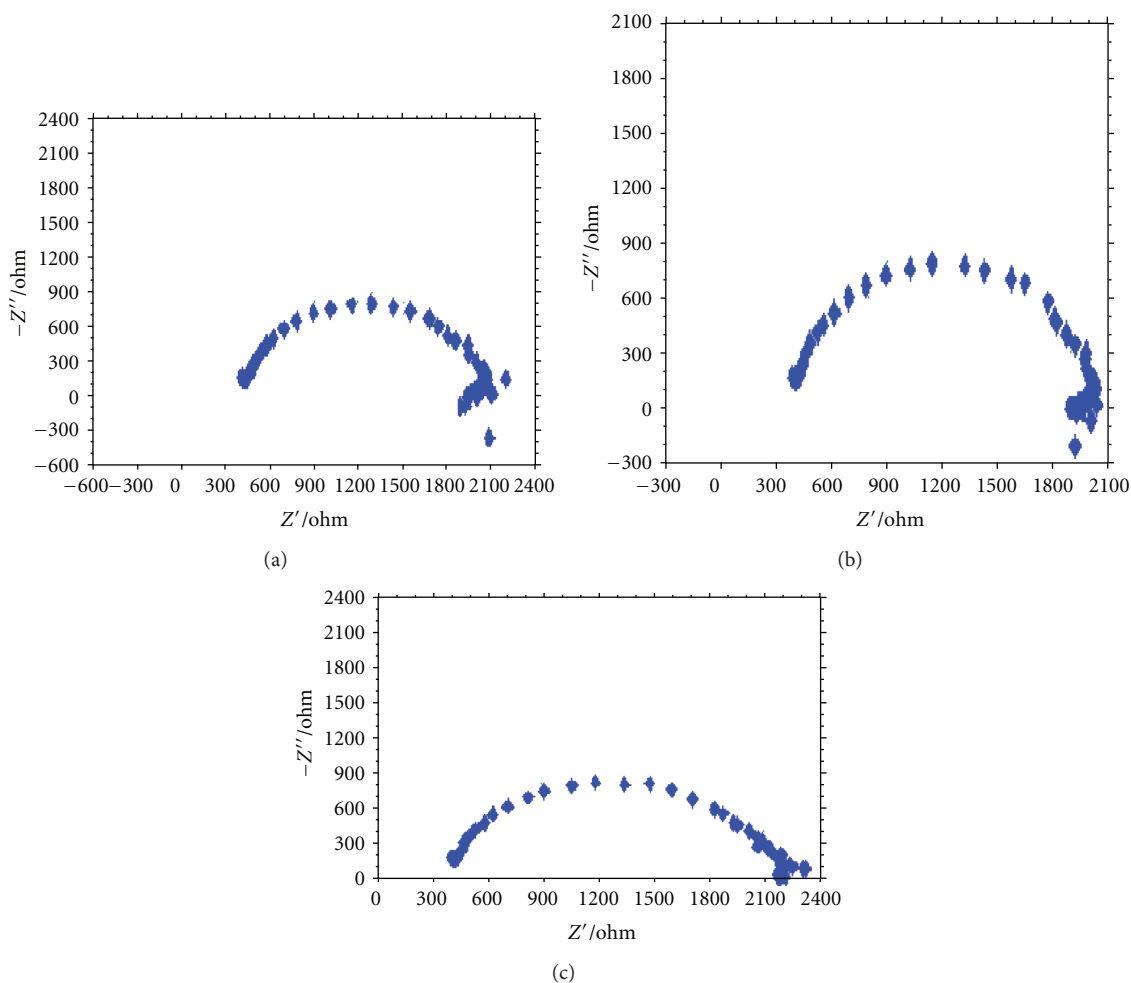


FIGURE 1: AC impedance spectra of carbon steel immersed in (a) well water, (b) caffeine (200 ppm) and  $\text{Zn}^{2+}$  (50 ppm), and (c) caffeine (200 ppm)- $\text{Zn}^{2+}$  (50 ppm)-malic acid (25 ppm).

The SEM images of magnification  $\times 1000$  of carbon steel specimen immersed in well water for 3 days in the absence and presence of inhibitor system are shown in Figures 4 and 5, respectively.

The SEM micrographs of polished carbon steel surface (control) in Figure 4 shows the smooth surface of the metal. This shows the absence of any corrosion products (or) inhibitor complex formed on the metal surface. The SEM micrographs of carbon steel surface immersed in well water (Figure 5(a)) shows the roughness of the metal surface which indicates the highly corroded area of carbon steel in well water. However Figures 5(b) and 5(c) indicates that in the presence of inhibitor (caffeine (200 ppm)- $\text{Zn}^{2+}$  (50 ppm), caffeine (200 ppm)- $\text{Zn}^{2+}$  (50 ppm)-malic acid (25 ppm) the rate of corrosion is suppressed, as can be seen from the decrease of corroded areas. The metal surface is almost free from corrosion due to the formation of insoluble complex on the surface of the metal. In the presence of inhibitor, the surface is covered by a thin layer of inhibitors which effectively controls the dissolution of carbon steel.

**3.6. Analysis of Results of Fluorescence Spectra.** Fluorescence spectra have been used to detect the presence of caffeine- $\text{Fe}^{2+}$  complex formed on the metal surface.

The emission spectrum ( $\lambda_{\text{ex}} = 300 \text{ nm}$ ) of solution containing caffeine- $\text{Fe}^{2+}$  complex prepared by mixing an aqueous solution of  $\text{Fe}^{2+}$  (prepared freshly from  $\text{FeSO}_4 \cdot 7 \text{H}_2\text{O}$ ) and caffeine is shown in Figure 6(a). A peak appears at 696 nm. It is concluded that the protective film consist of caffeine- $\text{Fe}^{2+}$  complex.

The emission spectrum ( $\lambda_{\text{ex}} = 300 \text{ nm}$ ) of the film formed on the metal surface after immersion in the solution containing, 200 ppm of caffeine and 50 ppm of  $\text{Zn}^{2+}$  is shown in Figure 6(b). A peak appears at 700 nm. This indicates that the protective film present on the metal surface consist of caffeine- $\text{Fe}^{2+}$  complex. The slight variation in the peak is due to the fact that the caffeine- $\text{Fe}^{2+}$  complex is entrained in  $\text{Zn}(\text{OH})_2$  present on the metal surface. Further the increase in intensity of the peak is due to the fact that the metal surface, after the formation of the protective film is very bright, the film is very thin, and there is enhancement in the intensity of the peak. The number of peak obtained is only one. Hence it



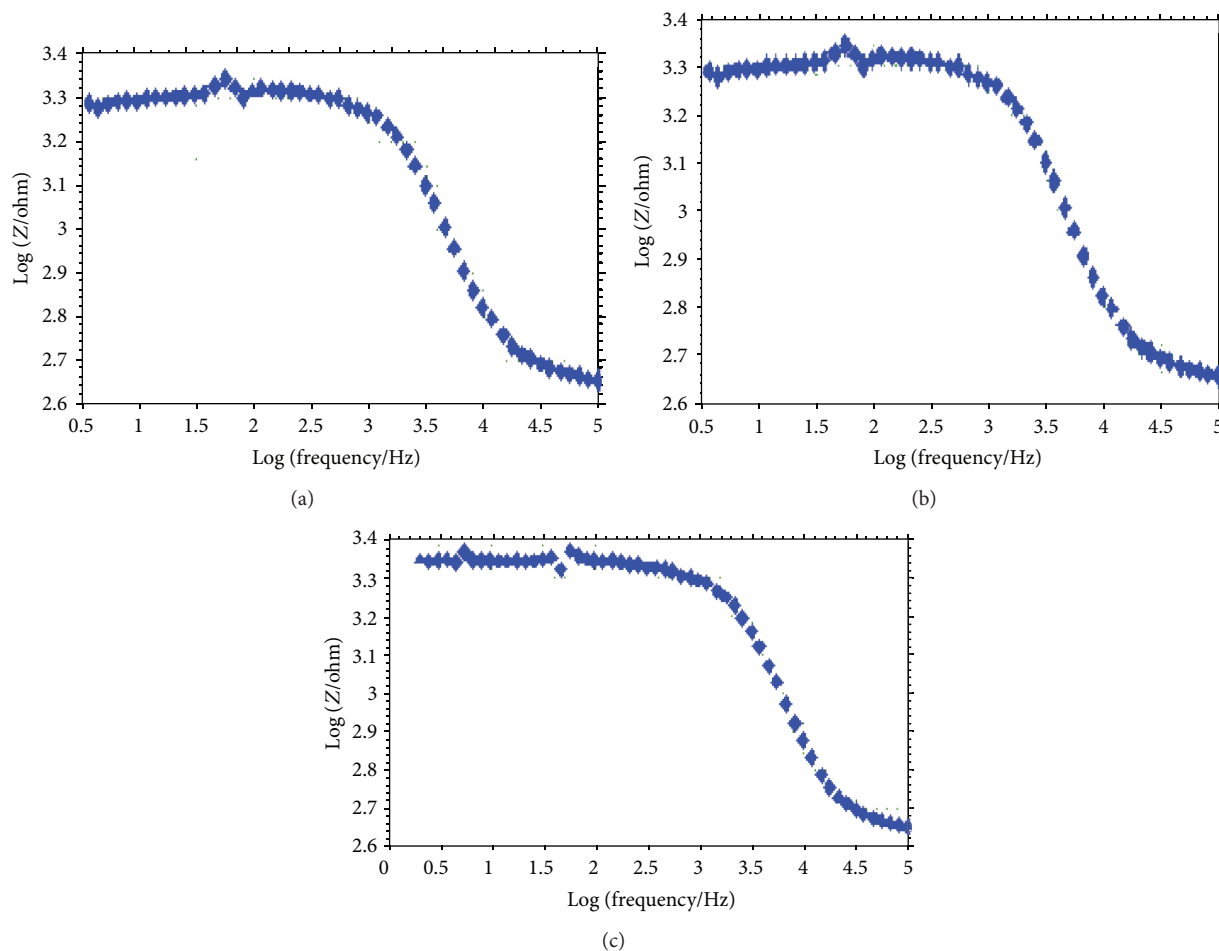


FIGURE 2: AC impedance spectra of carbon steel immersed in (a) well water (Blank) (Bode plot), (b) caffeine (200 ppm)- $\text{Zn}^{2+}$  (50 ppm) (Bode plot), and (c) Caffeine (200 ppm)- $\text{Zn}^{2+}$  (50 ppm)-malic acid (25 ppm) (Bode plot).

is inferred that the complex is of somewhat highly symmetric in nature.

The emission spectrum ( $\lambda_{\text{ex}} = 300 \text{ nm}$ ) of solution containing caffeine- $\text{Fe}^{2+}$ -malic acid complex is shown in Figure 7(a). A peak appears at 680 nm. It is concluded that the protective film consist of caffeine- $\text{Fe}^{2+}$ -malic acid complex.

The emission spectrum ( $\lambda_{\text{ex}} = 300 \text{ nm}$ ) of the film formed on the metal surface after immersion in the solution containing 200 ppm of caffeine, 50 ppm of  $\text{Zn}^{2+}$ , and 25 ppm of malic acid is shown in Figure 7(b). A peak appears at 690 nm. This indicates that the protective film present on the metal surface consist of caffeine- $\text{Fe}^{2+}$ -malic acid complex. The slight variation in the peak is due to the fact that the caffeine- $\text{Fe}^{2+}$ -malic acid complex is entrained in  $\text{Zn}(\text{OH})_2$  present on the metal surface. Further the increase in intensity of the peak is due to the fact that the metal surface, after the formation of the protective film is very bright, the film is very thin, and there is enhancement in the intensity of the peak.

It is concluded that the protective film consist of caffeine- $\text{Fe}^{2+}$ -malic acid complex. The number of peak obtained is only one. Hence it is inferred that the complex formed is of somewhat highly symmetric in nature.

#### 4. Analysis of FTIR Spectra

FTIR spectra of pure caffeine (Figure 8(a)) and the thin film formed on the surface of the carbon steel immersed in caffeine (200 ppm)- $\text{Zn}^{2+}$  (50 ppm) are shown in Figure 8(b). The FTIR spectrum of caffeine shows a broad peak at  $3408.42 \text{ cm}^{-1}$  due to N-H stretching vibration. Aromatic C-H stretch appears at  $3106.60 \text{ cm}^{-1}$  and  $2952.64 \text{ cm}^{-1}$ . The peak at  $1661.29 \text{ cm}^{-1}$  is due to  $-\text{C}=\text{N}$  ring stretching [26].

In the spectrum of film formed on the surface of carbon steel, the  $\text{C}=\text{O}$  stretching frequency has decreased from  $1661.29 \text{ cm}^{-1}$  to  $1637.45 \text{ cm}^{-1}$ . This is due to the shift of electron cloud of  $\text{C}=\text{O}$  bond towards  $\text{Fe}^{2+}$  ion formed on the metal surface. The band at  $1030.51 \text{ cm}^{-1}$  may be due to  $\text{Zn}-\text{O}$  stretching frequency. The band at  $1415.41 \text{ cm}^{-1}$  may be due to the in-plane vibration of O-H in  $\text{Zn}(\text{OH})_2$  [27]. The band at  $572.52 \text{ cm}^{-1}$  is due to the metal  $-\text{N/O}$  bonds [28]. All the above bands clearly indicate the formation of a complex. FTIR spectra of malic acid and caffeine (200 ppm)- $\text{Zn}^{2+}$  (50 ppm)-malic acid (25 ppm) is shown in Figure 9. The FTIR spectrum of malic acid Figure 9(a) shows a peak at  $3411.58 \text{ cm}^{-1}$  due to OH stretching. COOH stretching

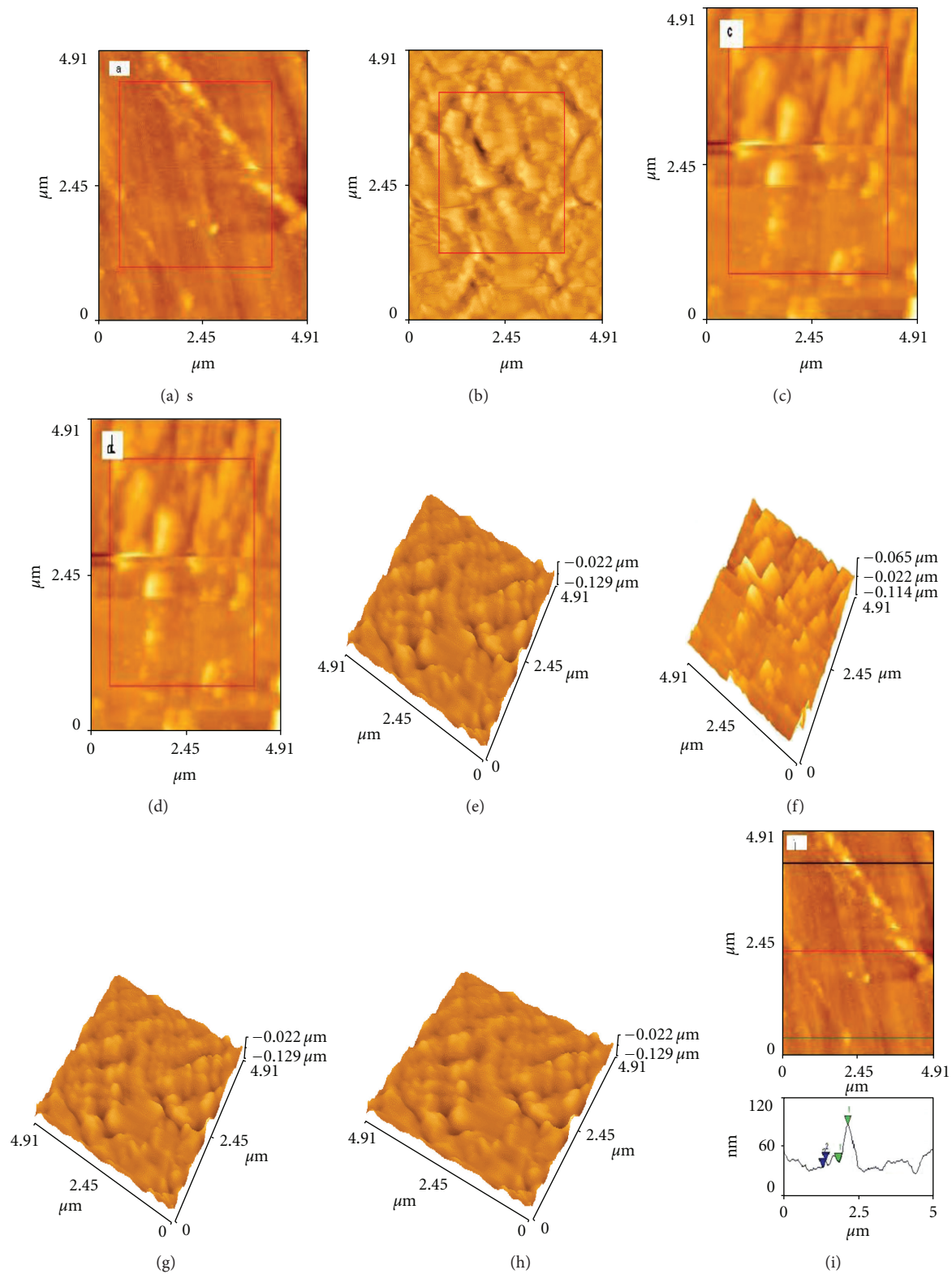


FIGURE 3: Continued.

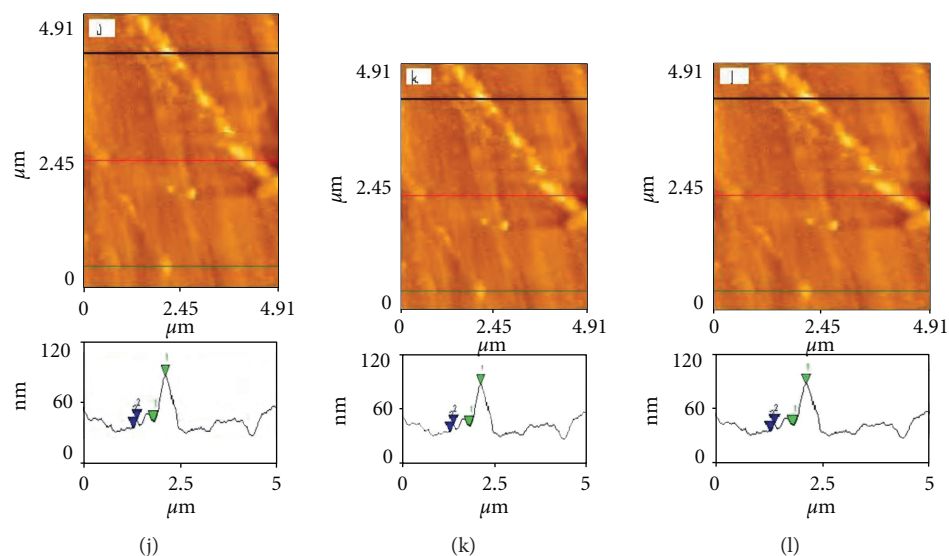


FIGURE 3: 2D AFM images of the surface of (a) polished carbon steel (control), (b) carbon steel immersed in well water (blank), (c) carbon steel immersed in well water containing caffeine (200 ppm)- $\text{Zn}^{2+}$  (50 ppm), and (d) carbon steel immersed in well water containing caffeine (200 ppm)- $\text{Zn}^{2+}$  (50 ppm)-malic acid (25 ppm). 3D AFM images of the surface of (e) polished carbon steel (control), (f) carbon steel immersed in well water (blank), (g) carbon steel immersed in well water containing caffeine (200 ppm)- $\text{Zn}^{2+}$  (50 ppm), and (h) carbon steel immersed in well water containing caffeine (200 ppm)- $\text{Zn}^{2+}$  (50 ppm)-malic acid (25 ppm). The cross sectional profiles, which are corresponding to as shown broken lines in AFM images of (i) polished carbon steel (control), (j) carbon steel immersed in well water (blank), (k) carbon steel immersed in well water containing caffeine (200 ppm)- $\text{Zn}^{2+}$  (50 ppm), and (l) carbon steel immersed in well water containing caffeine (200 ppm)- $\text{Zn}^{2+}$  (50 ppm)-malic acid (25 ppm).

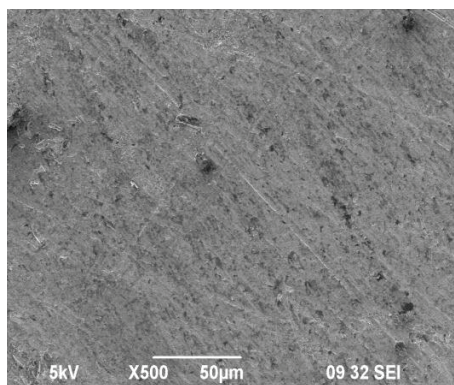


FIGURE 4: Carbon steel (control); magnification- $\times 500$ .

appeared at  $1722.1\text{ cm}^{-1}$ . FTIR spectrum of complex prepared by caffeine and malic acid is shown in Figure 9(b). The OH-stretching frequency is shifted to  $3448.06\text{ cm}^{-1}$  and C=O is shifted to  $1636.46\text{ cm}^{-1}$ . The band due to conjugated double bond shifts from  $3411.58\text{ cm}^{-1}$  to  $3448.06\text{ cm}^{-1}$ . All the above bands indicate the formation of a complex.

**4.1. Mechanism of Corrosion Inhibition.** Mass loss study reveals that the formulation consisting of 200 ppm caffeine + 50 ppm of  $\text{Zn}^{2+}$  + 25 ppm of malic acid offers 94% IE to carbon steel immersed in well water. AC impedance spectra, SEM micrographs, and AFM studies reveal the formation

of protective film on the metal surface. FTIR spectra reveal that the protective film consists of  $\text{Fe}^{2+}$ -caffeine complex and  $\text{Zn}(\text{OH})_2$ . The film is found to be UV fluorescent.

In order to explain the above facts in a holistic way, the following mechanism of corrosion inhibition is proposed.

- (i) When the formulation consisting of well water, caffeine and  $\text{Zn}^{2+}$  is prepared, there is formation of  $\text{Zn}^{2+}$ -caffeine complex in solution.
- (ii) When carbon steel is immersed in the solution, the  $\text{Zn}^{2+}$ -caffeine complex diffuses from the bulk of the solution towards the metal surface.



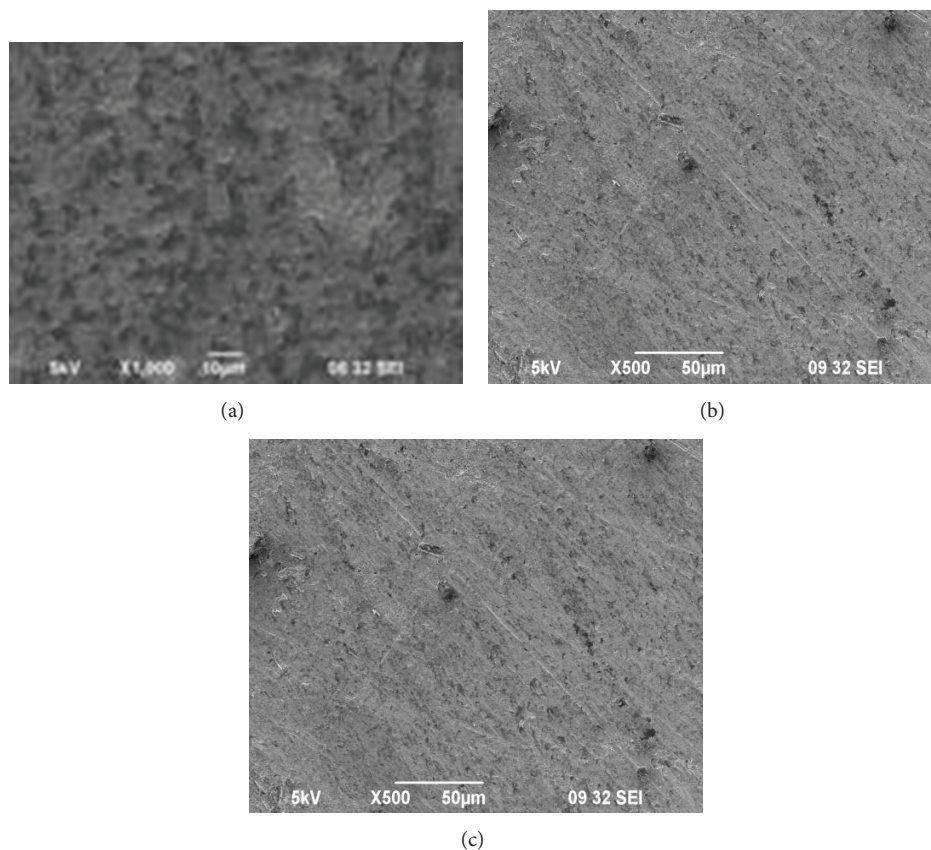


FIGURE 5: (a) Carbon steel in well water (Blank; Magnification- $\times 500$ ), (b) carbon steel in well water caffeine (200 ppm)- $\text{Zn}^{2+}$  (50 ppm) Magnification- $\times 500$ , and (c) carbon steel in well water caffeine (200 ppm)- $\text{Zn}^{2+}$  (50 ppm)-malic acid (25 ppm) Magnification- $\times 500$ .

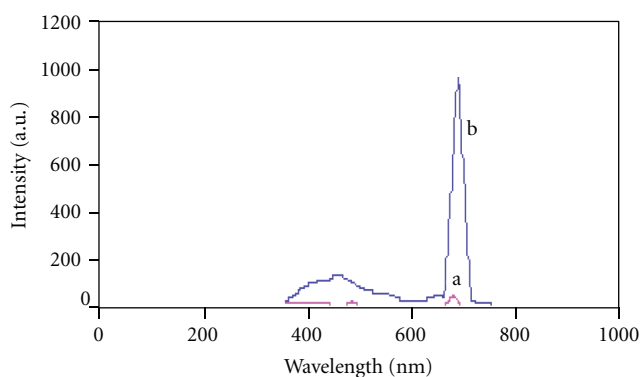


FIGURE 6: Fluorescence spectra of (a) caffeine- $\text{Fe}^{2+}$  complex in solution, (b) protective film formed on the metal surface of carbon steel after immersion in the solution containing 200 ppm of caffeine and 50 ppm of  $\text{Zn}^{2+}$ .

- (iii) On the metal surface,  $\text{Zn}^{2+}$ -caffeine complex is converted into  $\text{Fe}^{2+}$ -caffeine complex.  $\text{Zn}^{2+}$  is released.
- (iv)  $\text{Zn}^{2+}$ -caffeine +  $\text{Fe}^{2+} \rightarrow \text{Fe}^{2+}$ -caffeine +  $\text{Zn}^{2+}$ .
- (v) The released  $\text{Zn}^{2+}$  combines with  $\text{OH}^-$  to form  $\text{Zn}(\text{OH})_2$ .
- (vi)  $\text{Zn}^{2+} + 2 \text{OH}^- \rightarrow \text{Zn}(\text{OH})_2$ .
- (vii) Thus the protective film consists of  $\text{Fe}^{2+}$ -caffeine complex and  $\text{Zn}(\text{OH})_2$ .

## 5. Conclusions

The present study leads to the following conclusions:

- (i) the formulation consisting of 200 ppm of caffeine and 50 ppm of  $\text{Zn}^{2+}$  offers 82% inhibition efficiency to carbon steel immersed in well water;
- (ii) addition of malic acid increases inhibition efficiency of the caffeine- $\text{Zn}^{2+}$  system and 200 ppm caffeine,

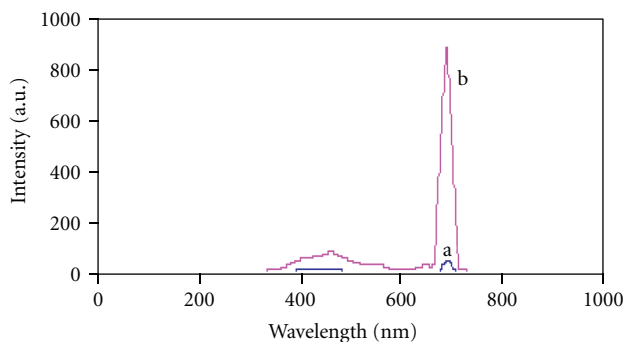


FIGURE 7: Fluorescence spectrum of (a) caffeine- $\text{Fe}^{2+}$ -malic acid complex in solution, (b) protective film formed on the metal surface of carbon steel after immersion in well water containing 200 ppm of caffeine, 50 ppm of  $\text{Zn}^{2+}$ , and 25 ppm of malic acid.

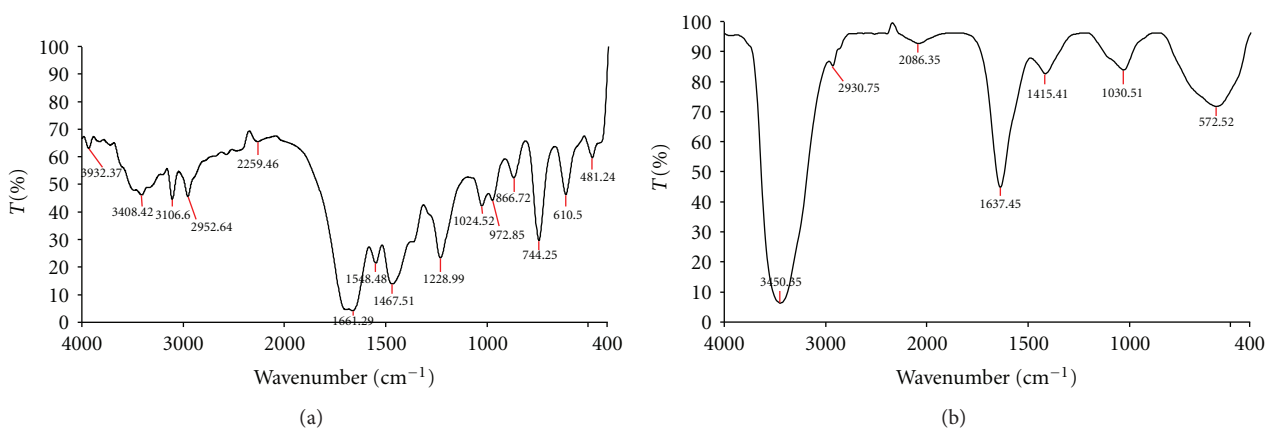


FIGURE 8: (a) FTIR spectra of caffeine, (b) FTIR spectra of caffeine- $\text{Zn}^{2+}$  complex.

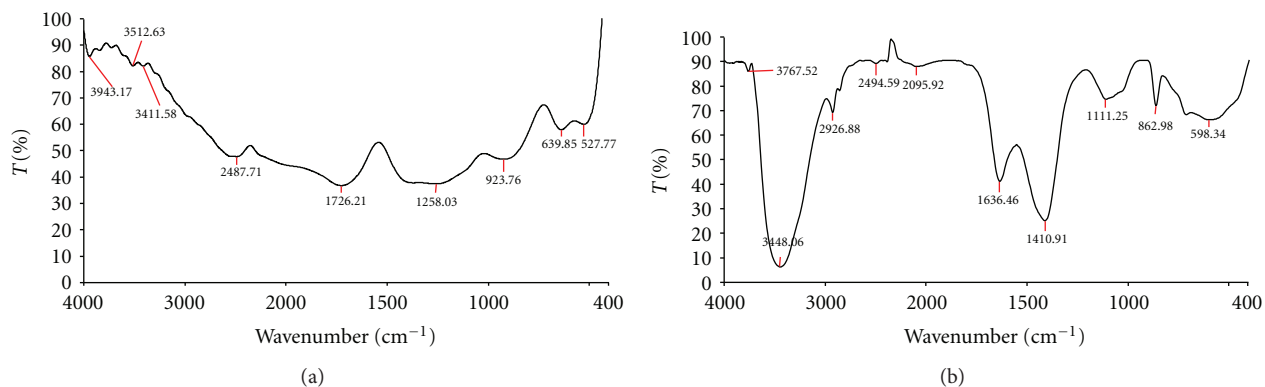


FIGURE 9: (a) FTIR spectra of malic acid, (b) FTIR spectra of caffeine- $\text{Zn}^{2+}$ -malic acid complex.

50 ppm of  $\text{Zn}^{2+}$  and 25 ppm of malic acid system offers 94% IE to carbon steel immersed in well water;

(iii) AC impedance spectra, SEM micrographs, and AFM studies reveal the formation of protective film on the metal surface;

(iv) FTIR spectra reveal that the protective film consists of  $\text{Fe}^{2+}$ -caffeine,  $\text{Fe}^{2+}$ -malic acid complex, and  $\text{Zn}(\text{OH})_2$ ;

(v) the film formed on the metal surface is found to be UV fluorescent.

## Acknowledgments

The authors are thankful to their Managements and University Grants Commission, India, for the help and encouragement and K. Rajam does not have any financial relation with the commercial identity.

## References

- [1] S. J. Zakvi and G. N. Mehta, "Corrosion inhibition of mild steel by pyridine derivatives," *Journal of the Electrochemical Society of India*, vol. 36, no. 3, pp. 143–145, 1987.
- [2] S. A. Abd El-Maksoud and A. S. Fouda, "Some pyridine derivatives as corrosion inhibitors for carbon steel in acidic medium," *Materials Chemistry and Physics*, vol. 93, no. 1, pp. 84–90, 2005.
- [3] B. Sathianandhan, K. Balakrishnan, and V. Subramaniam, "Triazoles as inhibitors of corrosion of mild steel in acids," *British Corrosion Journal*, vol. 5, no. 6, pp. 270–273, 1970.
- [4] J. P. Cotton and L. R. Scholes, "Benzotriazole and related compounds as corrosion inhibitors for copper," *British Corrosion Journal*, vol. 2, no. 1, pp. 1–5, 1967.
- [5] F. Mansfeld and T. Smith, "Benzotriazole as corrosion inhibitor for copper. II. Acid solutions," *Corrosion*, vol. 39, p. 105, 1973.
- [6] D. Tromans and J. C. Silva, "Anodic behavior of copper in chloride/tolytriazole and chloride/benzotriazole solutions," *Corrosion*, vol. 53, no. 1, pp. 16–25, 1997.
- [7] D. Altire and K. Nobe, "Hydrogen evolution on copper in  $\text{H}_2\text{SO}_4$  containing benzotriazole," *Corrosion*, vol. 28, no. 9, pp. 345–347, 1972.
- [8] G. W. Poling, "Reflection infra-red studies of films formed by benzotriazole on Cu," *Corrosion Science*, vol. 10, no. 5, pp. 359–370, 1970.
- [9] P. G. Fox, G. Lewis, and P. J. Boden, "Some chemical aspects of the corrosion inhibition of copper by benzotriazole," *Corrosion Science*, vol. 19, no. 7, pp. 457–467, 1979.
- [10] A. A. El-Hosary, R. M. Saleh, and H. A. El-Dahan, in *Proceedings of the 7th European Symposium on Corrosion Inhibitors*, University of Ferrara, Ferrara, Italy, 1970.
- [11] R. C. Pemberton, A. D. Mercer, E. J. Wright, and J. G. N. Thomas, in *Proceedings of the 6th European Symposium on Corrosion Inhibitors*, vol. 8, Ferrara, Italy, 1985.
- [12] S. Rajendran, S. Vaibhavi, N. Anthony, and D. C. Trivedi, "Transport of inhibitors and corrosion inhibition efficiency," *Corrosion*, vol. 59, no. 6, pp. 529–534, 2003.
- [13] S. Rajendran, A. J. Amalraj, M. J. Joice, N. Anthony, D. C. Trivedi, and M. Sundaravadivelu, "Corrosion inhibition by the caffeine— $\text{Zn}^{2+}$  system," *Corrosion Reviews*, vol. 22, no. 3, pp. 233–248, 2004.
- [14] A. M. Al-Mayouf, A. A. Al-Suhybani, and A. K. Al-Ameery, "Corrosion inhibition of 304SS in sulfuric acid solutions by 2-methyl benzoazole derivatives," *Desalination*, vol. 116, no. 1, pp. 25–33, 1998.
- [15] Y. Yesu Thangam, M. Kalanithi, C. M. Anbarasi, and S. Rajendran, "Inhibition of corrosion of carbon steel in a dam water by sodium molybdate— $\text{Zn}^{2+}$  system," *Arabian Journal for Science and Engineering*, vol. 34, no. 2C, pp. 49–60, 2009.
- [16] N. Anthony, E. Malarvizhi, P. Maheshwari, S. Rajendran, and N. Palaniswamy, "Corrosion inhibition by caffeine— $\text{Mn}^{2+}$  system," *Indian Journal of Chemical Technology*, vol. 11, no. 3, pp. 346–350, 2004.
- [17] G. Wranglan, *Introduction To Corrosion and Protection of Metals*, vol. 236, Chapman and Hall, London, UK, 1985.
- [18] S. Rajendran, A. J. Amalraj, M. J. Joice, N. Anthony, D. C. Trivedi, and M. Sundaravadivelu, "Corrosion inhibition by the caffeine— $\text{Zn}^{2+}$  system," *Corrosion Reviews*, vol. 22, no. 3, pp. 233–248, 2004.
- [19] S. Rajendran, B. V. Apparao, and N. Palaniswamy, "Synergistic effect of molybdate and  $\text{Zn}^{+2}$  on the Inhibition of corrosion of mild steel in neutral aqueous environment," *Journal of the Electro Chemical Society of India*, vol. 47, no. 1, pp. 43–48, 1998.
- [20] T. Fallavena, M. Antonow, and R. S. Gonçalves, "Caffeine as non-toxic corrosion inhibitor for copper in aqueous solutions of potassium nitrate," *Applied Surface Science*, vol. 253, no. 2, pp. 566–571, 2006.
- [21] F. S. de Souza and A. Spinelli, "Caffeic acid as a green corrosion inhibitor for mild steel," *Corrosion Science*, vol. 51, no. 3, pp. 642–649, 2009.
- [22] A. K. Satapathy, G. Gunasekaran, S. C. Sahoo, K. Amit, and P. V. Rodrigues, "Corrosion inhibition by *Justicia gendarussa* plant extract in hydrochloric acid solution," *Corrosion Science*, vol. 51, no. 12, pp. 2848–2856, 2009.
- [23] S. K. Selvaraj, A. J. Kennedy, A. J. Amalraj, S. Rajendran, and N. Palaniswamy, "Corrosion behaviour of carbon steel in the presence of polyvinylpyrrolidone," *Corrosion Reviews*, vol. 22, no. 3, pp. 219–232, 2004.
- [24] J. Sathiyabama, S. Rajendran, J. A. Selvi, and A. J. Amalraj, "Methyl orange as corrosion inhibitor for carbon steel in well water," *Indian Journal of Chemical Technology*, vol. 15, no. 5, pp. 462–466, 2008.
- [25] B. Shyamala Devi and S. Rajendran, *International Journal of Advances in Engineering Science and Technology*, vol. 1, no. 2, 2012.
- [26] R. M. Silverstein, G. C. Bassler, and T. C. Morrill, *Spectroscopic Identification of Organic Compounds*, John Wiley & Sons, New York, NY, USA, 1986.
- [27] V. C. Farmer, *The Infrared Spectra of Minerals*, Mineralogical Society, London, UK, 1974.
- [28] D. B. Powell and A. Woollins, "Vibrational spectra of metal, formamide complexes," *Spectrochimica Acta Part A*, vol. 41, no. 9, pp. 1023–1033, 1985.



